le.	**3. Report Type and Dates Covered.** Final - Proceedings

Model Diffuse Attenuation Coeffieient profiles

5. Funding Numbers.

Contract	
Program Element No.	0603741D
Project No.	P742
Task No.	
Accession No.	DN259069
Work Unit No.	9352ZA

6. Author(s).
L. Estep

7. Performing Organization Name(s) and Address(es).
Naval Oceanographic and Atmospheric Research Laboratory
Ocean Science Directorate
Stennis Space Center, MS 39529-5004

8. Performing Organization Report Number.
PR 92:044:352

9. Sponsoring/Monitoring Agency Name(s) and Address(es).
Naval Oceanographic and Atmospheric Research Laboratory
Ocean Acoustics and Technology Directorate
Stennis Space Center, MS 39529-5004

10. Sponsoring/Monitoring Agency Report Number.
PR 92:044:352

11. Supplementary Notes.
Published in IGARSS '92.

12a. Distribution/Availability Statement.
Approved for public release; distribution is unlimited.

12b. Distribution Code.

13. Abstract *(Maximum 200 words).*

Light transport through water is controlled by the properties of dissolved substances, particulate matter, and water itself. The rate at which the light field decays can be measured by optical instrumentation and parameterized by the apparent optical property of the water, the diffuse attenuation coefficient, k[1]. The diffuse attenuation coefficient is known to vary with depth near the surface[2]. However, as the light field penetrates to greater depths, the value of k approaches an asymptotic value which can be treated as a quasi-inherent property of the water mass[3]. Generally, the actual depth at which k approaches an asymptotic value is the bottom of the euphotic zone (1% level) for all but the clearest waters.

The primary optical parameter of interest in this study is the downwelling diffuse attenuation coefficient, k_d, which we will designate simply as "k". The objective of this work is to develop methods or algorithms for computing vertical, or depth, profiles of k given a surface k value.

14. Subject Terms.
Lasers, models, optics, surveillance

15. Number of Pages.
3

16. Price Code.

17. Security Classification of Report.	18. Security Classification of This Page.	19. Security Classification of Abstract.	20. Limitation of Abstract.
Unclassified	Unclassified	Unclassified	SAR

NSN 7540-01-280-5500

Standard Form 298 (Rev. 2-89)
Prescribed by ANSI Std. Z39-18
298-102

IGARSS '92

International Geoscience and Remote Sensing Symposium

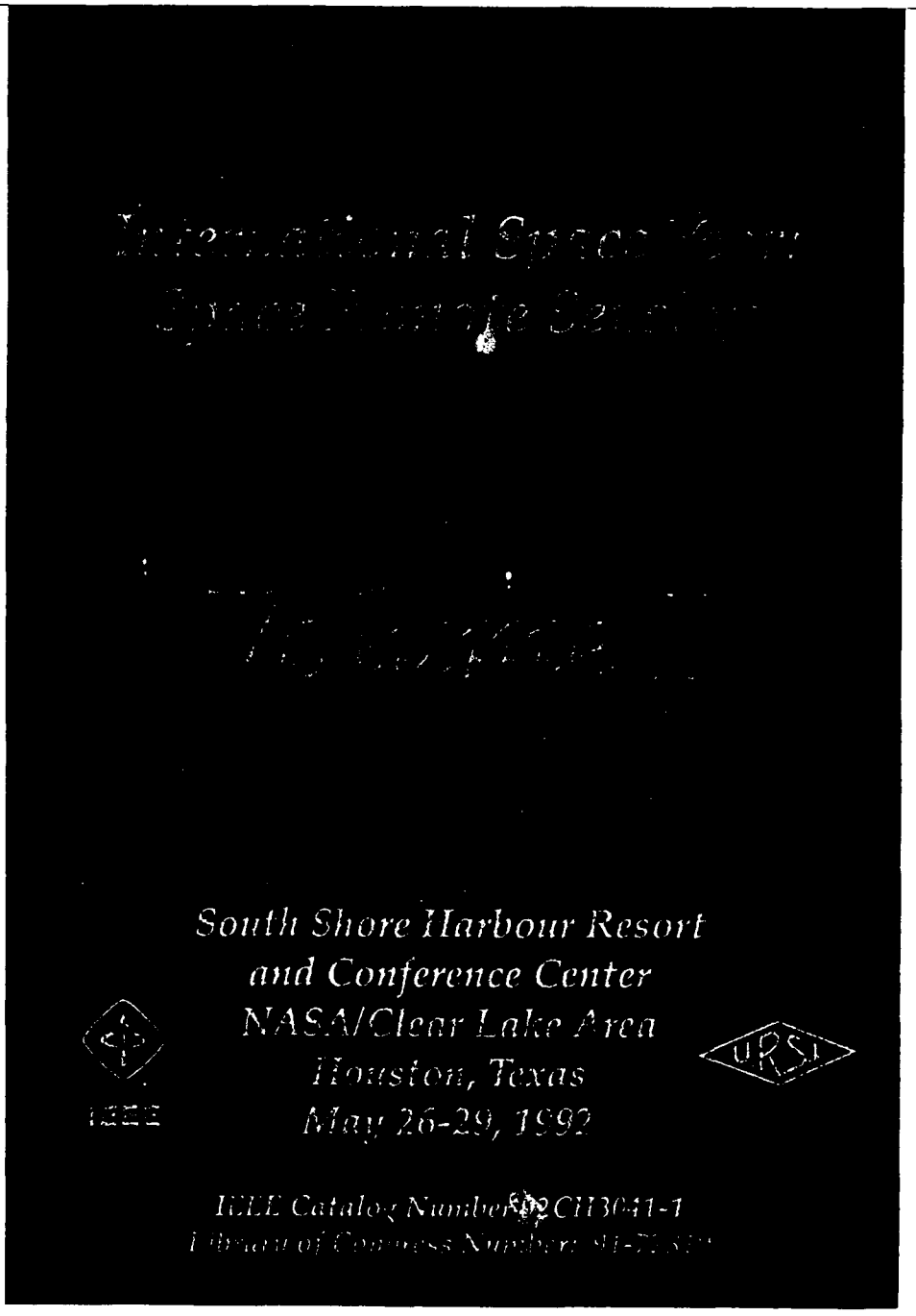

South Shore Harbour Resort
and Conference Center
NASA/Clear Lake Area
Houston, Texas
May 26-29, 1992

IEEE Catalog Number 92CH3041-1
Library of Congress Number 91-77[illegible]

MODEL DIFFUSE ATTENUATION COEFFICIENT PROFILES

L. Estep
Naval Research Laboratory
Stennis Space Center, MS. 39529.

INTRODUCTION

Light transport through water is controlled by the properties of dissolved substances, particulate matter, and water itself. The rate at which the light field decays can be measured by optical instrumentation and parameterized by an apparent optical property of the water, the diffuse attenuation coefficient, k[1]. The diffuse attenuation coefficent is known to vary with depth near the surface[2]. However, as the light field penetrates to greater depths, the value of k approaches an asymptotic value which can be treated as a quasi-inherent property of the water mass[3]. Generally, the actual depth at which k approaches an asymptotic value is the bottom of the euphotic zone (1% level) for all but the clearest waters.

The primary optical parameter of interest in this study is the downwelling diffuse attenuation coefficient, k_d, which we will designate simply as "k". The objective of this work is to develop methods or algorithms for computing vertical, or depth, profiles of k given a surface k value.

BACKGROUND AND METHODS

In Case I waters[4], a strong correlation has been shown to exist[5] between chlorophyll (Chl) concentration and water optics. Algorithms have been developed to allow transformations from chlorophyll concentrations in the surface ocean waters to k surface water optics. Using these algorithms in conjunction with satellite imagery, a synoptic view of the surface water optics of the world's oceans is possible. Case I surface waters comprise, on average, the top 15 to 20 meters of the ocean. The chlorophyll distribution with depth must be considered since it has been shown that values of surface water optics do not correlate with the water optical state with depth[6]. The focus of the present work has been to develop k profile algorithms that are locale specific.

Using results from several Scripps Institute of Oceanography cruises, Austin and McGlamery[7] developed relations between surface k values and the average k value over 100 meters and 200 meters depth. The relations are

$$\overline{k_{100}} = 0.307 k_s + 0.031, \qquad \overline{k_{200}} = 0.212 k_s + 0.031 \quad (1)$$

Using this information, a set of equations utilizing the diffuse optical depths invoked by the Austin and McGlamery results were derived. Figure 1 shows the profile development scenario.

The ocean from the surface to 200 meters depth is divided into three layers. These are termed the surface layer, the intermediate layer, and the bottom layer. Caution is advised in attempting to tie these layers to any actual oceanic layering in some given region. These layers are derived from purely

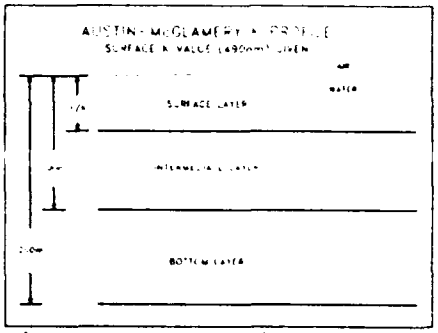

Figure 1. Austin-McGlamery model scenario.

statistical considerations over many different regions or sites. The surface layer has a satellite given k value of k_s and a thickness of $1/k_s$ m. The second, intermediate, layer is $100-1/k_s$ m thick and it's k_i value is given by the relation

$$k_i = \frac{100\overline{k_{100}} - 1}{100 - \frac{1}{k_s}} \quad (2)$$

The thickness of the bottom layer is 100 m and it's k_b value given by the formula

$$k_b = \frac{200\overline{k_{200}} - (100 - 1/k_s)k_i - 1}{100} \quad (3)$$

Thus, the surface-intermediate layer depth sum and bottom depth, are fixed in the model scenario. The k values of all three layers may vary depending on the surface k value given.

The second algorithm relies on some recent work by Platt et al.[8] that partitions the North Atlantic into a matrix based upon region, season, and water depth. These partitions provide specific Gaussian profile models for each element of the matrix to give the Chl distribution with depth. The Gaussian model used in this work has the form

$$C(z) = C_0 + \frac{h}{\sigma\sqrt{(2\pi)}} \exp\left[-\frac{(z-z_m)^2}{2\sigma^2}\right] \quad (4)$$

where C(z) represents the variation of Chl with depth, $h/(\sigma*(2*\pi)^{1/2})$ is the peak of the Chl maximum, C_0 is the background biomass upon which is superimposed the Gaussian profile, and σ is the width of the peak. The algorithm employed in the present work uses the Gaussian profile model above as well as the data for the width, peak value, and ratio of the peak to the background biomass, given by Platt et al.[8], to drive a local and surface specific Chl profile, which, in turn, is transformed back to a k value using results due to Morel[9]. The model takes as input a CZCS surface k value at 490 nm. This is transformed to a surface Chl value. Next, this surface Chl value is transformed using results due to Smith and Baker[10],

$$Log(C_t) = 0.7888\ Log(C_s) - 0.02 \quad (5)$$

91-72810/92$03.00 © IEEE 1992

where C_1 is the column averaged concentration, in mg/m^3, and C_s is the surface concentration. In Equation (1), the water depth over which the water column is taken is the euphotic depth, z_e. Thus, Smith and Baker's results provide us with a column average Chl value. The euphotic depth can be found from Morel[9] and is given by the relation

$$Z_{eu}=38.0Chl^{-0.428} \qquad (6)$$

where Chl is, here, the column average chlorophyll from the surface to the 1% light level. The product of the column averaged Chl over the euphotic depth and the euphotic depth gives an integrated Chl over the euphotic depth.

The next step is to calculate the background biomass, C_o. Integrating Equation (4) over the euphotic depth, using the peak to background biomass ratio, with C_o constant over the range of integration, we arrive at the form

$$C_o=\frac{Integrated\,Chl}{\int_0^{z_{eu}}\left[1+\rho\ \exp\left(-\frac{(z-z_m)^2}{2\sigma^2}\right)\right]dz} \qquad (7)$$

where "Integrated Chl" is the product of the column averaged Chl and euphotic depth aforementioned.

Given the values of the particular Platt partition, the algorithm determines the gaussian curve parameters. The algorithm then generates a profile which adjusts the parameters of the Gaussian profile peak to conserve total chlorophyll over the euphotic zone (or, in other words, bring Platt's results in line with references 9 and 10).

DATA COMPARISON RESULTS

Using field datasets obtained from the Sargasso Sea and the AUTEC range, comparisons were made with the algorithms mentioned above. Figures 2-5 give some comparisons of the k profile models of Austin-McGlamery, Platt, and the field data profiles.

Figure 2 exhibits line plots of the results of the Austin-McGlamery and Platt algorithms compared to AUTEC range data. The stair-step line shown above represents the downwelling k profile from field data. The legend labels the lines due to the two algorithms discussed above. Both the Austin-McGlamery and Platt results trend fairly close to the data line. However, the Platt results nearly lie on the data-line.

Figure 3 provides a field dataset where a deep chlorophyll maximum peak presents itself. The Platt and Austin-Morel models exhibit a peak, as does the data, but the peak phasing and amplitude are off. However, when one considers in all these cases that semi-empirical results from limited datasets are built into the models, it is not surprising that for some selected field dataset there will exist the sort of mismatch seen in Figure 3. In fact, it is rather surprizing that one can obtain the fairly close match seen in Figure 2.

Figure 4 and 5 provide further comparisons of the k profile model results compared to the field data.

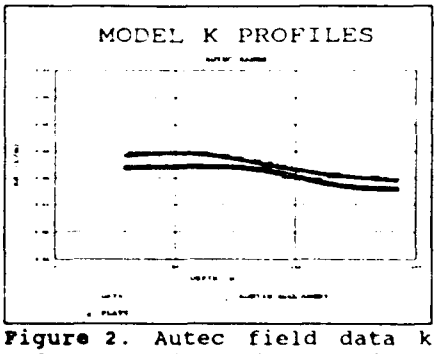

Figure 2. Autec field data k values plotted against algorithm results.

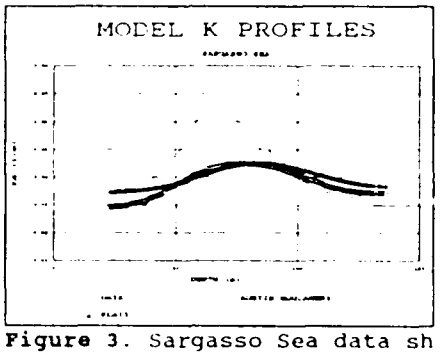

Figure 3. Sargasso Sea data showing a deep Chl maximum.

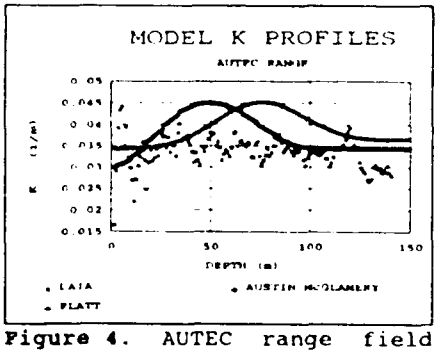

Figure 4. AUTEC range field results. Note scatter in k data.

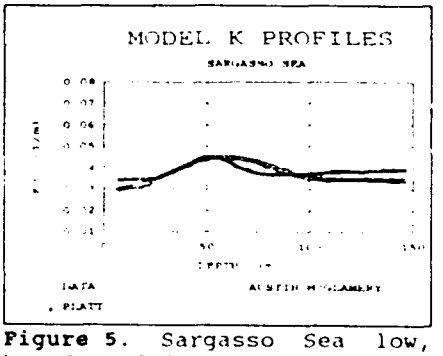

Figure 5. Sargasso Sea low, broad, and deep Chl peak.

Table 1 provides average error values for the deep water models versus the field data for the datasets shown above. The average error was calculated by computing the percent difference
error of the relevant model and associated field data results point by point and averaging over all points.

TABLE 1.
ERROR CALCULATION FOR DEEP WATER MODELS

AUSTIN–McCLAMERY	PLATT
38%	20%
5.5%	5%
15%	23%
16%	16%
AVG ERROR=18%	AVG ERROR=16%

Figure 6. Table of algorithm errors.

As seen in Table 1, their is little difference in the k profile algorithms in their relative accuracy of predicting real world profiles for the field data used.

CONCLUSIONS

Algorithms for the profiles of Chl or k with depth have been developed. These algorithms allow one to take surface values of downwelling k from satellite imagery and, without actual coeval supporting in situ measurements, derive a profile of k for a given pixel. These algorithms are confronted by field data. The algorithm that reproduces the deep water field data represented by the Sargasso Sea and AUTEC areas most closely is the Platt based model.

Caveats need to be made. First, the above work assumes Case I water scenarios. Second, the results are based upon work performed by extracting empirical relationships from real world datasets. If we can assume the datasets are generally representative of the world's oceans, then the profiles generated should provide representative estimates of the k profiles for areas of interest.

ACKNOWLEDGEMENTS

This work was supported by the SPAWARS ADI program. Dr. Gerald Morris program manager.

REFEERENCES

1. Duntley, S. Q., "Light in the Sea," J. Opt. Soc. Am., **58**, 214-233, 1963.
2. Preisendorfer, R. W., "Hydrologic Optics," vol.1, Washington: U.S. Department of Commerce, 1976.
3. Preisendorfer, R. W., "Hydrologic Optics," vol.3, Washington: U.S. Department of Commerce, 1976.
4. Morel, A., and L. Prieur, "Analysis of Variations in Ocean Color," Limnol. Oceanograph., **22**, pp.709-722, 1977.
5. Austin, R.W., and T.J. Petzold, " The determination of the diffuse attenuation coefficient of sea water using the coastal zone color scanner," Oceanography from Space, ed. J.F.R. Gower, Proceedings of COSPAR/SCOR/IUCRM Symposium, Venice 1980.
6. Mueller, J., "Bioptical provinces of the Northeast Pacific Ocean: A provisional analysis," Limnol. Oceanograph., **34**, pp.1572-1586, 1989.
7. Austin, R. W. and B. L. McGlamery, "Passive Remote Sensing of Ocean Optical Propagation Parameters," in Physical Aspects of Light in the Sea, ed. J. E. Tyler, Proceedings of Tenth Pacific Science Congress, Honolulu, HA, August 1961. University of Hawaii Press, 1964.
8. Platt, T., C. Caverhill, and S. Sathyendranath, "Basin-Scale Estimates of Oceanic Primary Production by Remote Sensing: The North Atlantic," Jour. Geophys. Res., **96**, 15147-15159, 1991.
9. Morel, A., "Optical Modeling of the Upper Ocean in Relation to Its Biogenous Matter Content (Case I Waters)," Journ. of Geophys. Res., **93**, 10749-10768, 1988.
10. Smith, R. C. and K. S. Baker, "The bio-optical state of ocean waters and remote sensing," Limnol. and Oceanog., **23**, 247-259, 1978.